

Chain-induced effects in the Faraday instability on ferrofluids in a horizontal magnetic field

V. V. Mekhonoshin* and Adrian Lange†
*Max-Planck-Institut für Physik komplexer Systeme,
Nöthnitzer Str. 38, D-01187, Dresden, Germany*
(Dated: November 11, 2018)

The linear stability analysis of the Faraday instability on a viscous ferrofluid in a horizontal magnetic field is performed. Strong dipole-dipole interactions lead to the formation of chains elongated in the field direction. The formation of chains results in a qualitative new behaviour of the ferrofluid. This new behaviour is characterized by a neutral stability curve similar to that observed earlier for Maxwell viscoelastic liquids and causes a significant weakening of the energy dissipation at high frequencies. In the case of a ferrofluid with chains in a horizontal magnetic field, the effective viscosity is anisotropic and depends on the field strength as well as on the wave frequency.

PACS numbers: 83.60.Bc, 83.60.Np, 83.60.Wc, 83.80.Hj, 47.20.Gv, 75.50.Mm

I. INTRODUCTION

Magnetic fluids (or ferrofluids) are colloidal dispersions of single domain nanoparticles in a carrier liquid. The fascination of ferrofluids stems from the combination of a normal liquid behaviour with the sensitivity to magnetic fields. This enables the use of magnetic fields to control the flow of the fluid, giving rise to a great variety of new phenomena and to numerous technical applications¹. One of the peculiarities of ferrofluids is the mutual influence of the microstructure and the rheological properties of the fluid. Due to strong interparticle interactions various aggregates can be formed in a ferrofluid^{2,3,4,5}. On the one hand, the formation of the aggregates changes the effective viscosity of the fluid. On the other hand, the motion of the fluid influences the structure of the aggregates.

In an applied magnetic field chains containing several particles are the favored form of an aggregate and are formed by the dipolar interactions. There is a similarity between the chains of dipoles and the macromolecular chains in polymer solutions. In both systems a network of chains is coupled with a viscous carrier liquid. This viscous coupling implies, that the relaxation character of the chain dynamics leads to a viscoelastic behaviour of the solution. The viscoelastic behaviour is reflected in a dependence of the stress tensor on the history of the system. The theoretical treatment of the viscoelasticity of polymer solutions is usually based on a phenomenological model. There are three well known models for an isotropic linear viscoelastic liquid. In the Maxwell model a viscoelastic element is a combination of a purely elastic spring with a purely viscous dashpot. In the Bingham two-component model these elements are connected parallel to each other, and the Jeffreys element is a superposition of the two previous ones. A comprehensive review of the theoretical basics and the existing models was done by Bird in Refs. 6,7. An overview of the theoretical approaches to the polymer dynamics is given by Doi and Edwards⁸.

A ferrofluid with chains in a magnetic field is an

anisotropic system. This makes it similar to a nematic liquid crystal (NLC), whose rheology can be described by a group of models usually referred as Ericksen-Leslie-Parody (ELP) models. The stress tensor in Refs. 9,10,11,12 involves five independent viscosity coefficients, which are scalar functions of the density and the temperature. ELP models are widely used in the hydrodynamics of NLC. These models were employed in the analysis of a flow instability¹³ and in studying periodic patterns¹⁴. In these papers as well as in Refs. 15,16 the influence of an external field was taken into account. Readers who are interested in a deeper insight into ELP models are referred to the books of de Gennes¹⁷ and Chandrasekhar¹⁸.

Since the susceptibility of ferrofluids is much higher than that of liquid crystals, the effects caused by external field should be more pronounced. The theoretical analysis of the rheology of a colloidal suspension containing ellipsoidal particles in a field was performed by Pokrovskij in Refs. 19,20. The model gives a constitutive equation of the ELP kind, where the viscosity coefficients are expressed in terms of the parameters of the suspension and the applied field. Electro- and magnetorheological fluids present a group of suspensions, whose behaviour is close to that of ferrofluids. The viscoelastic properties of electro- and magnetorheological fluids were studied experimentally in Refs. 21,22,23. Particularly it was shown that external fields can influence the rheological response of the fluid by changing the complex shear modulus and yield stress. Zubarev and Iskakova²⁴ used the results of Refs. 19,20 to obtain a constitutive equation for a ferrofluid with chains for the case of a weak flow of any kind. In the present paper the model suggested in Ref. 24 is applied to the linear stability analysis of the Faraday instability.

The Faraday instability denotes the parametric generation of standing waves on the free surface of a fluid subjected to vertical vibrations. The study of this phenomenon dates back to the observations by Faraday²⁵ in 1831. The initially flat free surface of the fluid becomes unstable at a certain intensity of the vertical vibrations of the whole system. As a result of the instability, a

pattern of standing waves is formed at the fluid surface. The typical response is subharmonic, i.e., the wave frequency is half the frequency of the excitation. A harmonic response can be observed on a shallow fluid at low frequencies²⁶. Faraday waves allows one to investigate symmetry breaking phenomena in a spatially extended nonlinear system. Therefore they experience a renewed interest in recent years. Detailed experimental studies of the various patterns on a viscous fluid have been performed^{27,28,29,30,31}, where a one-frequency as well as a two-frequency forcing were applied. Among the observed patterns are parallel rolls²⁷, hexagons²⁷, a twelve-fold quasi-pattern²⁷, triangles²⁸, superlattices formed by small and large hexagons²⁹, squares^{28,29,30,31}, and rhomboid pattern³¹.

The comprehensive linear stability analysis of the Faraday instability on an arbitrarily deep layer of a viscous non-magnetic fluid has been performed by Kumar and Tuckerman³². This analysis was tested experimentally³³ and an excellent agreement between the predicted and experimental data was found. In Refs. 26,34 the low frequency region is studied particularly. Bicritical points, where transitions from one type of response to others occur, are predicted and experimentally confirmed²⁶. In Ref. 35,36 an analogy between the Faraday instability and a periodically driven version of the Rayleigh-Taylor instability is exploited. Based on that analogy in Ref. 35 a scaling law is suggested, which satisfactorily describes the behaviour of the system in a wide range of parameters. S. Kumar³⁶ discusses the mechanism of the wave number selection in the Faraday instability on high-viscous fluids.

In our previous paper³⁷, the Faraday instability on a chain-free ferrofluid was studied. A nonmonotonic dependence of the stability threshold on the magnetic field is found at high frequencies of the vibrations. It was revealed that the magnetic field can be used to select the first unstable pattern of Faraday waves. In particular, a rhombic pattern as a superposition of two different oblique rolls can occur.

The Faraday instability of a viscoelastic non-magnetic liquid was studied experimentally in Ref. 38, where a harmonic response was detected. In Refs. 39,40,41 the Maxwell model of viscoelastic liquid was used in the theoretical analysis. The authors observed pronounced changes in the neutral stability curves. Particularly, the tongues related to the harmonic response became abnormal. Such a tongue has no tip and all tongues of higher order are inside this abnormal tongue.

The aim of the present paper is to investigate the role of the chains in the Faraday instability on a ferrofluid in a horizontal magnetic field. The formation of the chains leads to a dramatic increase of the magnetization relaxation time, changes the effective viscosity of the suspension, and increases the susceptibility of the ferrofluid. A number of model ferrofluids are investigated in a wide range of the parameters of the system to study the relative importance of those effects.

II. SYSTEM AND BASIC EQUATIONS

A. Model

A dielectric, viscous, and incompressible magnetic fluid with constant density ρ is considered, which contains particles of the equal size. The strength of the dipole-dipole interactions is characterized by the coupling constant $\varepsilon = \mu_0 m^2 / (16\pi R^3 k_B T)$, which is the ratio of the energy of interaction between two particles at the minimal separation with head-to-tail orientation of their magnetic moments to the thermal energy. Here $m = 4M_s \pi R_0^3 / 3$ is the magnetic moment of a particle, $R = R_0 + \delta$ is the hydrodynamic radius of the particle, M_s is the magnetization of the magnetic material, R_0 is the radius of the magnetic core of a particle, δ is the thickness of the nonmagnetic layer, k_B is the Boltzmann constant, and T is the temperature. The interaction of a particle with the applied field H is measured by the Langevin parameter $\kappa = \mu_0 m H / (k_B T)$. In the case of a magnetic fluid with low particle volume fraction φ , interactions between chains can be neglected. Assuming that the chains are straight and rigid, Zubarev and Iskakova determined the size distribution of chains, which minimizes the free energy of such a magnetic fluid and is given by²⁴:

$$g_n = \frac{x^n \sinh(\kappa n)}{v \kappa n} \exp(-\varepsilon), \quad (1)$$

$$x = \left[2y \cosh \kappa + \sinh \kappa - \sqrt{(2y \cosh \kappa + \sinh \kappa)^2 - 4y^2} \right] / (2y),$$

where v is the volume of a particle and $y = \kappa \varphi \exp(\varepsilon)$. Each chain containing n particles is modelled by an uniaxial ellipsoid with semi-axes equal to nR and R . This keeps the solid phase volume density unchanged and allows one to use the results of Pokrovskij^{19,20}. The viscous stress tensor for a system of uniaxial ellipsoids consists of a symmetric and antisymmetric part

$$\sigma_{ik} = \sigma_{ik}^{(s)} + \sigma_{ik}^{(as)}, \quad (2)$$

where

$$\begin{aligned} \sigma_{ik}^{(s)} = & 2\eta \gamma_{ik} + \eta \\ & \times \left\langle \left\langle \left[2\alpha_n \gamma_{ik} - \rho_n \langle e_j e_s \rangle_n \delta_{ik} \gamma_{js} \right. \right. \right. \\ & + (\zeta_n + \beta_n \lambda_n) (\langle e_i e_j \rangle_n \gamma_{jk} + \langle e_k e_j \rangle_n \gamma_{ji}) \\ & + \beta_n (\Omega_{ij} \langle e_j e_k \rangle_n + \Omega_{kj} \langle e_j e_i \rangle_n) - \beta_n \frac{d}{dt} \langle e_i e_k \rangle_n \\ & \left. \left. \left. + (\chi_n - 2\lambda_n \beta_n) \langle e_i e_k e_j e_s \rangle_n \gamma_{js} \right] \right\rangle \right\rangle, \\ \sigma_{ik}^{(as)} = & \frac{\kappa k_B T}{2v} \langle \langle \langle e_i \rangle_n - \langle e_k \rangle_n h_i \rangle \rangle. \end{aligned}$$

Both parts contain the geometric factors $\alpha_n, \beta_n, \chi_n, \lambda_n, \rho_n$, and ζ_n , which are entirely determined by the aspect ratio of an ellipsoid corresponding to a n -particle chain^{19,20,24,42}. η is the viscosity of the carrier liquid, $\gamma_{ik} = (\partial_k u_i + \partial_i u_k)/2$ and $\Omega_{ik} = (\partial_k u_i - \partial_i u_k)/2$ are the symmetric and antisymmetric parts of the tensor of velocity gradients, \mathbf{e} and $\mathbf{h} = \mathbf{H}/H$ are the unit vectors along the chain axis and the magnetic field, and the following notations are used:

$$\langle\langle \dots \rangle\rangle = \sum_n \dots n \nu g_n,$$

$$\langle \dots \rangle_n = \int \dots \mathbf{e} \psi_n(\mathbf{e}) d\mathbf{e}, \quad \langle \dots \rangle_n^0 = \int \dots \mathbf{e} \psi_n^0(\mathbf{e}) d\mathbf{e}.$$

Here, $\psi_n^0(\mathbf{e})$ and $\psi_n(\mathbf{e})$ are the equilibrium and the nonequilibrium angular distribution functions. The former is known due to the classical Langevin model and the latter is the solution of the Fokker-Planck equation (see Refs. 19,20,24). The exact solution for the case of an arbitrary field is unknown. Therefore, Zubarev and Iskakova suggested an approximation for $\psi_n(\mathbf{e})$:

$$\psi_n(\mathbf{e}) = \psi_n^0(\mathbf{e}) \left[1 + a_i (e_i - \langle e_i \rangle_n^0) + b_{ik} (e_i e_k - \langle e_i e_k \rangle_n^0) \right], \quad (3)$$

where \mathbf{a} and \overleftrightarrow{b} are a vector and a symmetric tensor. They can be found from the equations for the first $\langle e_k \rangle_n$ and the second $\langle e_i e_k \rangle_n$ moments of $\psi_n(\mathbf{e})$, which are derived from the Fokker-Planck equation^{19,20,24} with the accuracy up to the linear terms with respect to the velocity gradients. The moment equations for $\langle e_k \rangle_n$ and $\langle e_i e_k \rangle_n$ involve two relaxation times, $\tau_1 = 1/(2D)$ and $\tau_2 = 1/(6D)$, where $D \sim 1/\eta$ is the coefficient of rotational diffusion.

One can easily see, that the magnetization of the ferrofluid is

$$\mathbf{M} = M_s \frac{R_0^3}{R^3} \langle\langle \langle \mathbf{e} \rangle_n \rangle\rangle. \quad (4)$$

If \mathbf{a} and \overleftrightarrow{b} are known one can relate the viscous stress tensor $\overleftrightarrow{\sigma}$ and the magnetization to the tensor of velocity gradients for the given value of magnetic field strength \mathbf{H} . The total stress tensor \overleftrightarrow{T} reads

$$T_{ik} = - \left(p + \mu_0 \int_0^H M dH' + \frac{\mu_0}{2} H^2 \right) \delta_{ik} + H_i B_k + \sigma_{ik}, \quad (5)$$

where $\mathbf{B} = \mu_0 (\mathbf{H} + \mathbf{M})$, p is the pressure, and \mathbf{B} the induction of the magnetic field.

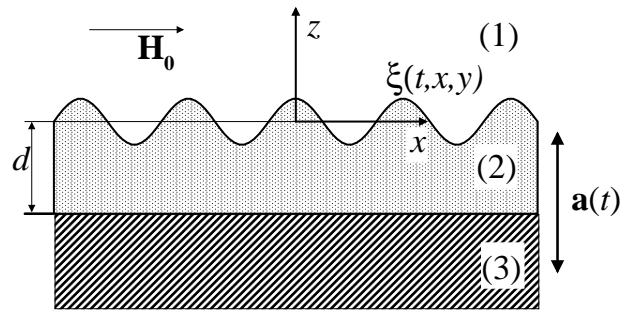


FIG. 1: A horizontally unbounded ferrofluid layer (2) is placed in a nonmagnetic container (3) with air (1) above. The system is subjected to a horizontal magnetic field \mathbf{H}_0 and harmonic vertical vibrations $\mathbf{a}(t)$.

B. The system

The above model is used to analyze the stability of the free surface of a ferrofluid in the following setup. The laterally infinite ferrofluid layer of arbitrary depth d is subjected to a homogeneous dc horizontal magnetic field $\mathbf{H}_0 = (H_0, 0, 0)$ and harmonic vertical vibrations (Fig. 1). The plane $z = 0$ coincides with the nondeformed surface of the ferrofluid. The fluid layer is bounded from below by the bottom of the nonmagnetic container and has a free surface described by $\xi(t, x, y)$ with air above.

Due to zero electrical conductivity of the fluid, the static form of the Maxwell equations is used for the magnetic field in all three media. The fluid motion is governed by the continuity equation and the conservation law of the linear momentum

$$\text{div } \mathbf{u} = 0, \quad (6a)$$

$$\rho \left[\frac{\partial u_i}{\partial t} + (\mathbf{u} \text{ grad}) u_i \right] = \partial_j T_{ij}^{(2)} - \rho g(t) \delta_{i,3}, \quad i = 1, 2, 3. \quad (6b)$$

The vertical vibrations add a periodic term to the gravity acceleration \mathbf{g}_0 , i.e., a modulated value $\mathbf{g}(t) = (0, 0, -g_0 - a \cos(\omega t))$ appears in the equations of the fluid motion. Here a is the acceleration amplitude and ω is the angular frequency of the vibrations. The governing set of equations has to be supplemented by the boundary conditions, which are the same as in Ref. 37.

III. LINEAR STABILITY ANALYSIS

Following the standard procedure^{32,43}, the governing equations and the boundary conditions have been linearized in the vicinity of the nonperturbed state

$$\mathbf{u} = 0, \quad \xi = 0, \quad \mathbf{H}^{(i)} = \mathbf{H}_0, \quad i = 1, 2, 3,$$

$$p_0 = p^{(1)} - \frac{\mu_0}{2} M_0 H_0 - g(t)z,$$

where M_0 and p_0 are the magnetization and the pressure in the unperturbed state. In order to construct the linearized governing equations for the small perturbations, which encompass the magnetic field strength \mathbf{H}_1 , the pressure p_1 , and a nonzero velocity \mathbf{u} of the fluid, it is necessary to expand all quantities in Taylor series.

The above defined distribution functions g_n and ψ_n are affected by the small perturbations. Since the formation and the dissociation of chains are connected with the diffusion of particles in the suspension, they are rather slow processes. It can be estimated by the Schmidt number $Sc = \eta/(\rho D_0)$ which relates the characteristic time for mass transport by flow to the characteristic time for mass transport by diffusion. For a typical ferrofluid the Schmidt number is about $5 \cdot 10^6$ with $\eta = 0.1$ kg/(ms), $\rho = 1020$ kg/m³, and the Brownian diffusion coefficient $D_0 = 2 \cdot 10^{-11}$ m²/s⁴⁴. Therefore we neglect the changes in g_n caused by the perturbations. This implies that the size distribution of chains does not depend either on the spatial coordinates or on time. In Refs. 19,20,24 only spatially homogeneous systems are considered. An extension to the case of a spatially inhomogeneous system results in additional convective terms in the dynamic equations for ψ_n [Eq. (12) in Ref. 24]. Since these terms are of the form $(\mathbf{u} \text{ grad}) \psi_{n,1}$, i.e., they are of second order with respect to the perturbations, they can be neglected in a linear stability analysis. As long as the typical length scale of a chain ($\sim 10^{-8} \dots 10^{-7}$ m) is smaller than that of the spatial variation of the perturbations (typically $\sim 10^{-3} \dots 10^{-2}$ m), Zubarev's model can be applied in the present setup. Our results (see Sec. IV) suggest that this condition is always fulfilled.

The symmetry of the system possesses a number of restrictions on \mathbf{a} and \overleftrightarrow{b} . The change of y to $-y$ and z to $-z$ should not change the components a_x , b_{xx} , b_{yy} , and b_{zz} , whereas this transformation leads to the change of a sign of the components a_y , a_z , b_{xy} , and b_{xz} . This completes the set of the moment equations derived from the Fokker-Planck equation^{19,20,24}, and gives us the values of \mathbf{a} and \overleftrightarrow{b} .

After \mathbf{a} and \overleftrightarrow{b} are found, we have for the perturbations \mathbf{M}_1 of the magnetization and those of the total stress tensor $\overleftrightarrow{T}_1^{(2)}$:

$$\begin{aligned} M_{1x} &= A_1 \gamma_{xx} + A_2 H_{1x}^{(2)} \\ M_{1y} &= A_3 \gamma_{xy} + A_4 \Omega_{xy} + A_5 H_{1y}^{(2)} \\ M_{1z} &= A_3 \gamma_{xz} + A_4 \Omega_{xz} + A_5 H_{1z}^{(2)} \\ T_{1xx}^{(2)} &= -p_1 + A_6 \gamma_{xx} + A_7 H_{1x}^{(2)} \\ T_{1xy}^{(2)} = T_{1yx}^{(2)} &= A_8 \gamma_{xy} + A_9 \Omega_{xy} + A_{10} H_{1y}^{(2)} \\ T_{1xz}^{(2)} = T_{1zx}^{(2)} &= A_8 \gamma_{xz} + A_9 \Omega_{xz} + A_{10} H_{1z}^{(2)} \\ T_{1yy}^{(2)} &= -p_1 + A_{11} \gamma_{xx} + A_{12} \gamma_{yy} + A_{13} H_{1x}^{(2)} \\ T_{1yz}^{(2)} = T_{1zy}^{(2)} &= A_{12} \gamma_{yz} \\ T_{1zz}^{(2)} &= -p_1 + A_{11} \gamma_{xx} + A_{12} \gamma_{zz} + A_{13} H_{1x}^{(2)}, \end{aligned}$$

where A_1, A_2, \dots, A_{13} are known functions of the applied magnetic field, the frequency of the vibrations, as well as of the parameters of the ferrofluid, and the equation of continuity in the form $\gamma_{xx} + \gamma_{yy} + \gamma_{zz} = 0$ has been used. The functions A_i are obtained by means of averaging (with function $\psi_n(\mathbf{e})$) over the orientations of chains and averaging over the sizes of the chains (with function g_n).

Thus, the set of governing equation for the first order of the perturbations can be written:

$$\text{div } \mathbf{B}_1^{(i)} = 0, \quad \text{rot } \mathbf{H}_1^{(i)} = 0, \quad i = 1, 2, 3, \quad (7a)$$

$$\text{div } \mathbf{u} = 0, \quad (7b)$$

$$\rho \frac{\partial u_i}{\partial t} = \partial_j T_{1ij}^{(2)}. \quad (7c)$$

Here \mathbf{B}_1 is the perturbation of the induction of the magnetic field.

The linearized boundary conditions differ from those in Ref. 37 by the condition for continuation of the stress tensor across the free surface of the fluid

$$n_j (T_{1ij}^{(1)} - T_{1ij}^{(2)}) - \delta_{i,3} \sigma \Delta_{\perp} \xi = 0 \quad i = 1, 2, 3 \quad \text{at } z = 0, \quad (8)$$

where $\Delta_{\perp} = \partial_{xx} + \partial_{yy}$. In contrast to the previous case³⁷, the first two equations in (8) are independent of each other.

The stability of the flat surface with respect to standing waves is analyzed by using the Floquet ansatz for the surface deformations and the z -component of the velocity

$$\xi(t, x, y) = \sin(\mathbf{k}\mathbf{r}) e^{(s+i\alpha\omega)t} \sum_{n=-\infty}^{\infty} \xi_n e^{in\omega t}, \quad (9a)$$

$$u_z(t, x, y, z) = \sin(\mathbf{k}\mathbf{r}) e^{(s+i\alpha\omega)t} \sum_{n=-\infty}^{\infty} w_n(z) e^{in\omega t}, \quad (9b)$$

where $\mathbf{k} = (k_x, k_y, 0)$ is the wave vector, s is the growth rate, and α is the parameter determining the type of the

response. For $\alpha = 0$ the response is harmonic whereas for $\alpha = 1/2$ it is subharmonic. Expansions similar to (9b) are made for all other small perturbations and are inserted into the linearized governing equations (7). The functions of the vertical coordinate in the Floquet expansion are of the form $w_n(z) = C_w e^{\pm qz}$, where C_w is a complex amplitude of the corresponding quantity. The condition of reality for $\xi(t, x, y)$ leads to the equations³²

$$\xi_{-n} = \xi_n^*, \quad \alpha = 0, \quad (10a)$$

$$\xi_{-n} = \xi_{n-1}^*, \quad \alpha = 1/2. \quad (10b)$$

Inserting the ansatz into the governing equations (7), we obtain a set of algebraic equations for the amplitudes of all perturbed quantities. The solvability condition for this set gives us four values of the modified wave vector q . Hence, the general solution of the set of governing equations in the ferrofluid contains eight arbitrary constants. Two more arbitrary constants are the amplitudes of the perturbations of the field in the air above and below the fluid after applying the boundary conditions at $z \rightarrow \pm\infty$. Ten of the boundary conditions [Eqs. (8) and (3.2a)-(3.2f) in Ref. 37] allow one to express all the perturbed quantities in terms of the coefficients ξ_n which satisfy the equation

$$\sum_{n=-\infty}^{\infty} (W_n \xi_n - a \xi_{n-1} - a \xi_{n+1}) e^{[s+i(\alpha+n)\omega]t} = 0, \quad (11)$$

where W_n are rather complicated functions of the applied field, the frequency of vibrations, the depth of the fluid layer, and of the parameters of the ferrofluid. Here the functions W_n depend additionally on the coupling constant ε in contrast to the corresponding functions in the previous paper³⁷.

Equation (11) has to be satisfied for all times which implies that each term of the sum equals to zero. Using the relations between ξ_n with positive and negative numbers (10), one gets the set of equations

$$W_0 \xi_0 - a \xi_1^* - a \xi_1 = 0, \quad \alpha = 0, \quad (12a)$$

$$W_0 \xi_0 - a \xi_0^* - a \xi_1 = 0, \quad \alpha = 1/2, \quad (12b)$$

$$W_n \xi_n - a \xi_{n-1} - a \xi_{n+1} = 0, \quad n = 1, \dots, \infty. \quad (12c)$$

A cutoff at $n = N$ (in the present work $N = 100$) leads to a self-consistent equation for the acceleration amplitude a ^{45,46},

$$a = |F(a, k, \omega, H_0, \eta, \sigma, \rho, \kappa, \varepsilon)|, \quad (13)$$

where F is a complex function expressed in terms of continued fractions. Equation (13) can be solved numerically and gives the dependence of a on k at fixed parameters. The critical values of the acceleration amplitude a_c and the wave number k_c correspond to the absolute minimum of the curve $a(k)$ at zero growth rate ($s = 0$).

IV. RESULTS AND DISCUSSION

Figure 2 presents marginal stability curves for a viscous ferrofluid at high frequency for two cases. The dashed lines are calculated with neglect of the magnetization relaxation time, $\mathbf{a} = 0$ and $\mathbf{b} = 0$, i.e. the average orientation of chains immediately follows the field perturbations. The solid lines depict the neutral stability curves for the system out of equilibrium. The dependence of the acceleration amplitude on the wave number for $s = 0$ divides the phase space into regions, where the surface of the ferrofluid is stable or unstable with respect to parametrically driven standing waves. The principal data, which can be extracted, are the critical acceleration amplitude (scaled with g_0), the critical wave number (scaled with the capillary wave number $k_\sigma = \sqrt{\rho g / \sigma}$), and the number of the tongue to which they belong. The number of a tongue l (from left to right) is the order of response: the basic wave frequency related to the l -th tongue is $\omega_l = l\omega/2$. The odd and even tongues are the regions, where either a subharmonic or a harmonic instability develops. That relation for the different instability types holds for Newtonian ferrofluids³⁷ but experiences significant changes if the ferrofluid contains chains.

Due to the finite relaxation time the tongues are deformed. All tongues but one are now shaped by a lower boundary, a pronounced tip, and an upper boundary. For the chosen set of parameters in Fig. 2 the fourth tongue becomes exceptionally deformed, since it has no tip and no upper boundary in the way all other tongues have. It is caused by the fact that the self-consistent equation for the acceleration amplitude (13) has always a solution as k goes to infinity. To note the difference to all

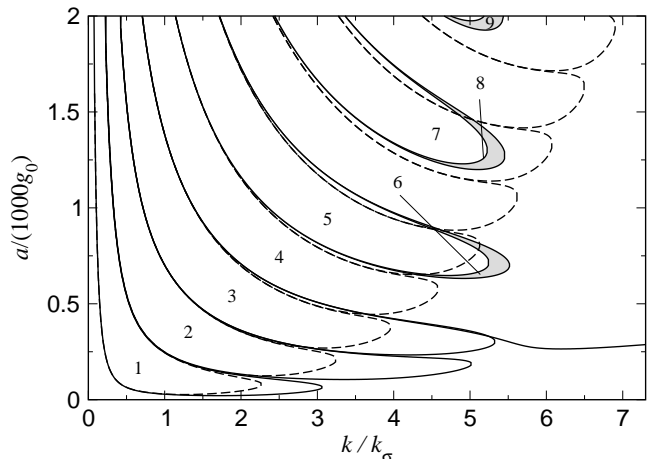


FIG. 2: Neutral stability curves for the excitation frequency $f = 100$ Hz and layer depth $d = 5$ mm. Dashed (solid) lines are calculated with (without) taking into account deviations of the magnetization from equilibrium. The parameters of the fluid are $\eta = 0.1$ kg/(ms), $\varepsilon = 5$, $\kappa = 0.5$, $\sigma = 0.0265$ N/m, $\rho = 1020$ kg/m³, $R = 10.5$ nm, $k_\sigma = 614.5$ m⁻¹, and the particle volume fraction $\varphi = 0.082$.

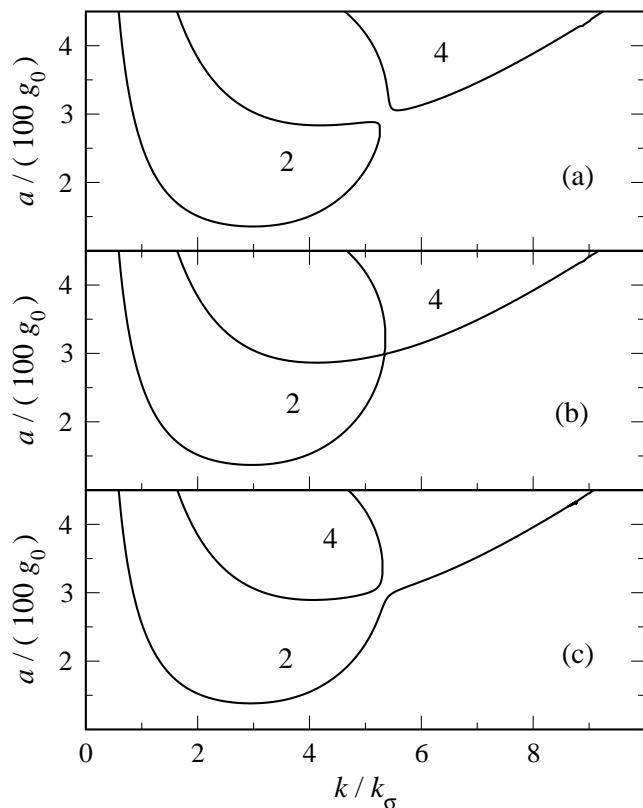


FIG. 3: The second and the fourth tongues of the neutral stability curves for the viscosities of the carrier liquid $\eta = 0.136$ kg/(ms) (a), $\eta = 0.138$ kg/(ms) (b), and $\eta = 0.14$ kg/(ms) (c). The remaining parameters are the same as in Fig. 2.

other deformed tongues, we call it a abnormal tongue because this tongue lacks two essential features in comparison with all other tongues⁴⁷. The typical arrangement of tongues in Fig. 2 can be generalized as follows: it is always an even tongue, $l_{\text{abno}} = 2N$, $N = 1, 2, \dots$, which becomes abnormal (here $l_{\text{abno}} = 4$). All tongues with $l > l_{\text{abno}}$ form separated pairs of two overlapping tongues (here $l = 5, 6$ and $l = 7, 8$) inside the abnormal tongue. All tongues corresponding to a higher order harmonic response, $l = l_{\text{abno}} + 2L$, $L = 1, 2, \dots$, are "islands" of stability with respect to a response of the system with the frequency ω_{abno} . In the domains, where the subharmonic tongues overlap with the regions of the harmonic type of instability (gray regions in Fig. 2), both types of instability can occur.

Figure 3 illustrates the scenario of the transition between the neutral stability curves with $l_{\text{abno}} = 4$ and $l_{\text{abno}} = 2$ with an increase of the viscosity of the carrier liquid. At the point, where two tongues touch each other, the amplitudes for the corresponding terms in the Floquet ansatz (9) become equal. The number of the abnormal tongue l_{abno} depends on the mean relaxation time of a chain $\tau_0 = 1/\langle\langle 2D \rangle\rangle$. The latter can be varied by changing the viscosity of the carrier liquid η . In the

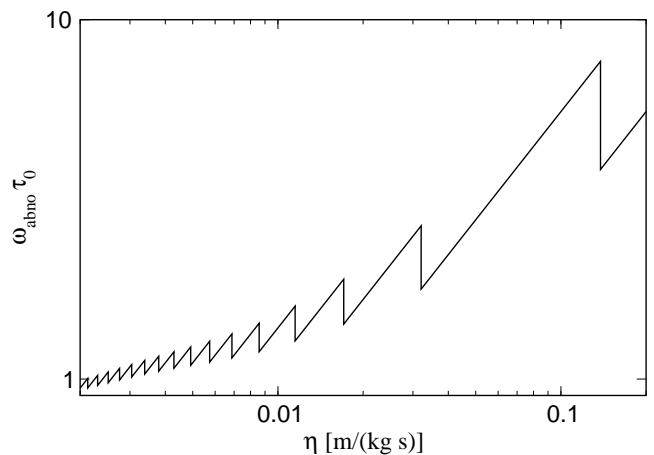


FIG. 4: Dependence of the product $\omega_{\text{abno}}\tau_0$ (see text) on the viscosity of the carrier liquid. The remaining parameters are $\varepsilon = 5$, $\kappa = 0.3$, $\sigma = 0.0265$ N/m, $\rho = 1020$ kg/m³, $R = 10.5$ nm and $\varphi = 0.082$.

figure 4, the product $\omega_{\text{abno}}\tau_0$ is presented as a function of η . As the relaxation time increases with the viscosity, the corresponding number l_{abno} decreases: from $l_{\text{abno}} = 60$ for $\eta = 0.001$ kg/(ms) to $l_{\text{abno}} = 4$ for $\eta = 0.1$ kg/(ms). Therefore sequential changes of the number of the abnormal tongue occur. The corresponding value of $\omega_{\text{abno}}\tau_0$ shows a jump-like decrease at those points, where l_{abno} drops to $l_{\text{abno}} - 2$.

Both the overlapping of tongues and the appearance of an abnormal one were also observed for the Maxwell viscoelastic liquid^{39,40}, and it seems that these features are signs of a viscoelastic behaviour. One has to note that if the angular distribution of chains is assumed to be in equilibrium (dashed lines in Fig. 2), i.e. $\tau_0 = 0$, the neutral stability curves are standard tongues without any qualitative changes in comparison with the case of a Newtonian ferrofluid (studied in Ref. 37). It shows that it is the combination of chains *and* their nonzero mean relaxation time which causes the new features in the neutral stability curve.

The dependencies of the critical wave number and the critical acceleration amplitude on the *excitation frequency* $f = \omega/2\pi$ are presented in Fig. 5. The curves denoted by *A* are calculated for a nonequilibrium magnetization and the curves *B* present the case, where the chains follow the field perturbations immediately. The solid lines correspond to the ferrofluid layer with depth $d = 5$ mm, and the dashed lines are calculated for an infinitely deep layer. It is seen that at high frequencies the critical acceleration in the system out of equilibrium is lower than that in a model system, where the relaxation time is neglected. It is clear that with a decrease of the frequency the deviations of the magnetization from an equilibrium and their importance become smaller. Therefore, one can expect that curves *A* and *B* coincide at low frequencies. However, this is observed only in the case of the infinitely deep fluid layer. In

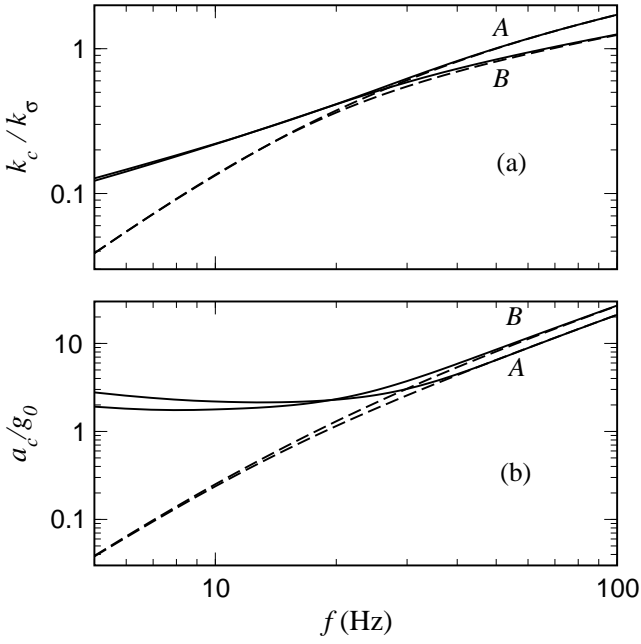


FIG. 5: Frequency dependencies of the critical wave number k_c (a) and the critical acceleration amplitude a_c (b) for $d = 5$ mm (solid lines) and $d = \infty$ (dashed lines). The magnetization is assumed to be out of equilibrium for curves A and in equilibrium for curves B. The remaining parameters are the same as in Fig. 2.

the case of $d = 5$ mm, the finiteness of the layer and consequently the influence of the viscous stresses in the bottom fluid layer become stronger in the case of the system out of equilibrium, and the critical acceleration increases more rapidly with a decrease of the frequency. With the further decrease of the frequency, transitions to higher order response occur^{26,34,37}, and the frequency of the Faraday waves remains high enough to leave the orientation of chains in nonequilibrium.

Fig. 6 presents the relative differences between the critical parameters $k_c^{(\text{free})}$ and $a_c^{(\text{free})}$ for a chain-free ferrofluid and those for a ferrofluid with chains as functions of the Langevin parameter, i. e., of the dimensionless magnetic field. The magnetization, chord $\chi_c = M/H$, and differential susceptibility $\chi_d = \partial M / \partial H$ of the chain-free ferrofluid are chosen the same as in the ferrofluid with chains at each point. The magnetization is out of equilibrium in the ferrofluid with chains and is in equilibrium in the chain-free one. It is seen, that at $f = 20$ Hz the formation of the chains decrease the critical wave number [curve A in Fig. 6(a)]. Since the stresses at the bottom layer are essential at this frequency and $d = 2$ mm, this leads to the increase of the critical acceleration amplitude [curve A in Fig. 6(b)]. At the higher frequency, $f = 100$ Hz, the changes of k_c are non-monotonic. There is a range of the parameters, where the critical wave number on the ferrofluid with chains is larger than that on the chain-free ferrofluid. The critical acceleration amplitude is decreased by the formation of chains [curve B in

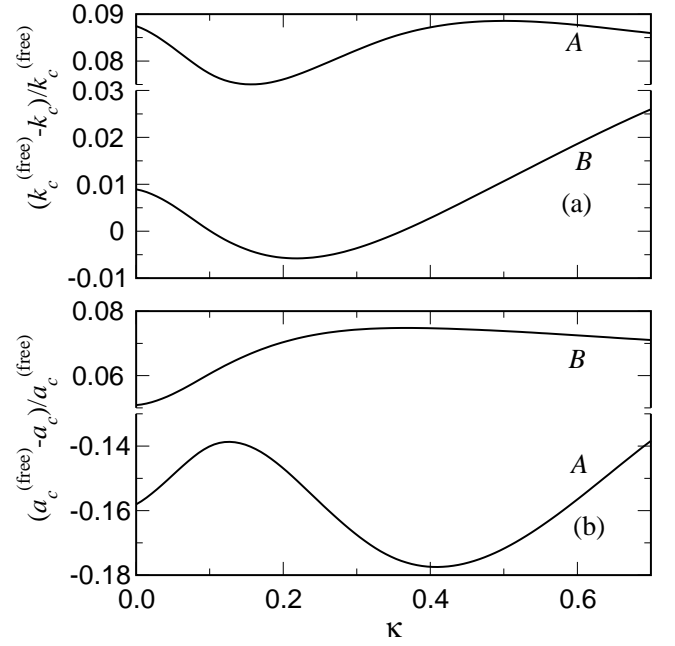


FIG. 6: The relative differences between the critical wave numbers (a) and the critical acceleration amplitudes (b) as functions of the Langevin parameter. The quantities with the superscript “(free)” belong to the chain-free ferrofluid ($g_n = \delta_{n,1} \varphi / v$), the quantities without a superscript belong to the ferrofluid with chains [g_n is given by Eq. (1)]. Curve A: $f = 20$ Hz, curve B: $f = 100$ Hz. The layer depth is $d = 2$ mm and the remaining parameters are the same as in Fig. 2.

Fig. 6(b)]. Note, that the susceptibility of the ferrofluid changes strongly with the increase of the field, therefore the relative importance of the influences of the magnetic field, the fluid microstructure, and the viscous stresses depends on the field.

The above results were obtained for the particular case $\mathbf{k} \parallel \mathbf{H}_0$. The typical size and orientation of chains depend on the applied field. Therefore, the threshold of the instability depends on the strength of the field and the angle θ between \mathbf{k} and \mathbf{H}_0 separately. It is not possible to introduce a single parameter like the effective field³⁷, which would incorporate those two dependencies. This fact is illustrated in Fig. 7. The product $H_0 \cos \theta$ was varied in two ways. For the curves indicated by A, the field strength was changed from zero to $H_{0\text{max}} = 1.46$ kA/m with $\theta = 0$. In the second case (curves B), θ was changed from zero to $\pi/2$ at the constant field $H_{0\text{max}}$. In contrast to the chain-free ferrofluid studied in Ref. 37, where both curves would be identical, there are now two different graphs. Whereas the critical wave numbers have similar values for the two ways of variation, the critical acceleration shows greater differences: for instance for $H_0 \cos \theta / H_{0\text{max}} = 0.5$ the difference in k_c is 0.4 % against 2.5 % for a_c . Thus it makes a notable difference for the stability of the free surface whether the system is subjected to ($\theta = 0, H_0 = H_{0\text{max}}/2$) or to ($\theta = 60^\circ, H_0 = H_{0\text{max}}$). This fact suggests a simple

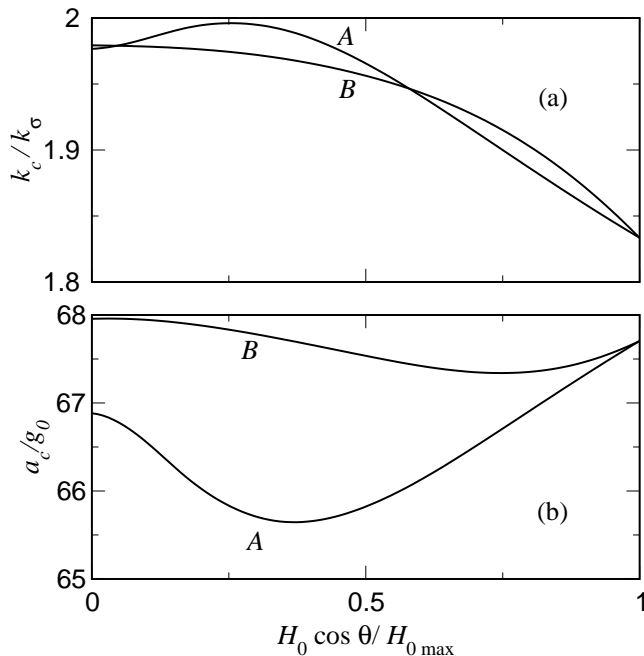


FIG. 7: The dependencies of the critical wave number (a) and the critical acceleration amplitude on the projection of \mathbf{H}_0 on the direction of \mathbf{k} for $f = 100$ Hz and $d = 1$ mm. The curve A is obtained by varying the field strength with $\theta = 0$, whereas the curve B was calculated by varying θ with $H_0 = H_{0\max} = 1.46$ kA/m. Remaining parameters are the same as in Fig. 2.

method to test the presence of chains in a sample. If the ferrofluid is chain-free both ways of excitation lead to the same value of a_c , if it contains chains one gets two different values.

The dependencies are less pronounced than in the previous case, where $H_{0\max} = 26.6$ kA/m³⁷, due to the fact that the range of rather weak fields is studied here. Such a choice of fields ensures that $\langle n \rangle \leq \varepsilon$ and that the head-to-tail orientation of the moments in a chain is still preferable which is needed to apply the model.

The nonmonotonic dependence of $a_c(H_0)$ for $\theta = 0$ [curve A in Fig. 7(b)] caused by the joint action of the two mechanisms of the viscous damping: i) the dissipation in the bulk fluid and ii) the viscous stresses in the bottom fluid layer. The first mechanism is dominant for large wave numbers and causes a decrease of a_c . The second becomes important with the decrease of the wave number and results in an increase of a_c with field strength. A detailed discussion of this nonmonotonic behaviour of $a_c(H)$ is given in Ref. 37.

There are three effects caused by the formation of chains. Since a chain has a magnetic moment larger than that of a single particle, the formation of chains leads to the increase of the magnetization of the system at the given field in comparison with a homogeneous ferrofluid. This strengthens the field influence on the fluid motion. The effect can be formally taken into account by adjust-

ing the magnetization and susceptibility of the chain-free ferrofluid in such a way as it is done in Fig. 6. The two other effects are more interesting. The chains increase the magnetization relaxation time and change the effective viscosity of the suspension both in a steady and in a periodical flow^{19,20,24}.

In order to investigate the role of these two effects, a number of model ferrofluids are considered. The first sample is a ferrofluid with chains. It is characterized by the mean relaxation time of a chain τ_0 and unperturbed values of the magnetization M_0 as well as the chord χ_c and the differential susceptibility χ_d . The second model ferrofluid contains as well chains, but in this case the relaxation time is neglected [$\psi_n(\mathbf{e}) = \psi_n^0(\mathbf{e})$]. The third and the fourth ferrofluid is chain-free ($g_n = \delta_{n,1}\varphi/v$) with the same unperturbed values of M_0 , χ_c , and χ_d . The magnetization relaxation time for the third ferrofluid is equal to τ_0 , and for the fourth sample the relaxation time is neglected, i.e. the last sample is the ferrofluid, which was studied in Ref. 37. The predictions of the Zubarev model for the case of a chain-free ferrofluid with a finite relaxation time were compared with the results of a model using the effective field theory developed by Martsenyuk, Raikher, and Shliomis in 1974⁴⁸. In the both cases, the Langevin parameter κ_{adj} involved in the model was adjusted to obey $m\varphi/vL(\kappa_{adj}) = M_0$, where $L(\kappa) = \coth(\kappa) - 1/\kappa$ denotes the Langevin function. A fairly good agreement between the threshold parameters predicted by both models is observed. In Figure 8 the coupling constant ε is varied by changing the temperature. The intensity of the applied magnetic field H_0 is changed in such a way that the Langevin parameter is equal to $\kappa = 0.5$.

The comparison of the presented dependencies reveals that the finiteness of the magnetization relaxation time leads to an increase of the critical wave number [compare the pairs of the curves A – C and B – D in Fig. 8(a)]. At the same time, the changes in the slow-flow rheological properties of the suspension caused by the formation of the chains decrease strongly the critical wave number (compare curves C – D and A – B). The net effect of those two influences gives the behaviour that is presented by the curves B in Fig. 8.

The critical acceleration amplitude for a ferrofluid with nonequilibrium chains [curve B in Fig. 8(b)] has the lowest value among all the tested model ferrofluids. This can be interpreted as a sign of an elastic behaviour, which is typical for viscoelastic liquids at high frequencies. This fact is confirmed in Fig. 9, where the real and the imaginary parts of the effective viscosity $\eta_{\text{eff}} = [\sigma_{ik}/(2\gamma_{ik}\eta) - 1]/\varphi$ of a ferrofluid are presented as functions of the frequency of surface waves $f_l = \omega_l/(2\pi)$ with $l = 1$. The case $H_0 = 0$ is considered, where the system is isotropic and the influence of the chains on the rheological properties of the suspension can be characterized by the single complex parameter η_{eff} ²⁴. The real part of the effective viscosity determines the dissipation of the energy in the system, and a nonzero imaginary part leads

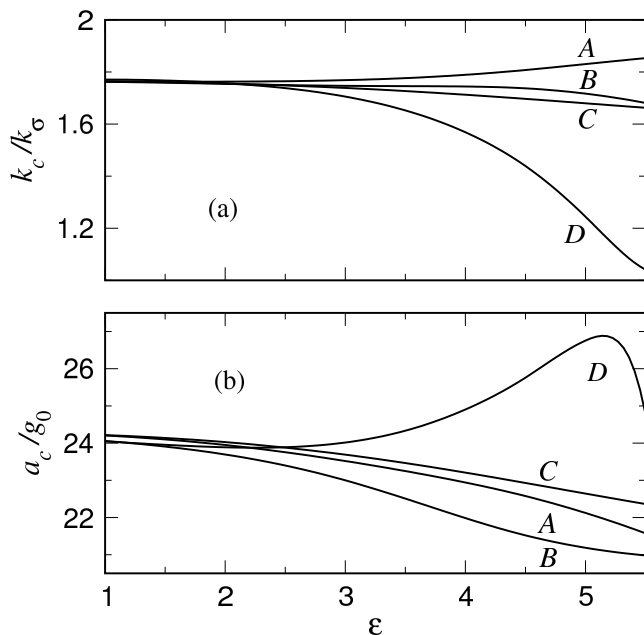


FIG. 8: The dependencies of the critical wave number (a) and the critical acceleration amplitude for the infinitely deep layer of the ferrofluid consisting of *A*: single particles with the Brownian relaxation time $\tau_B = \tau_0$; *B*: chains with a orientations out of equilibrium [Eq. (3)]; *C*: single particles with zero relaxation time; *D*: chains with the equilibrium orientations [$\psi_n(\mathbf{e}) = \psi_n^0(\mathbf{e})$]. The remaining parameters are the same as before.

to a phase shift between the tensor of velocity gradients and the stress tensor, i.e. to a viscoelastic behaviour. It is seen that the imaginary part of the effective viscosity is nonzero and has a maximum at a frequency of $f_l \simeq 5$ Hz [solid line in Fig. 9(b)], where therefore a maximal phase shift (viscoelastic behaviour) can be expected. At the same time, the real part of the effective viscosity decreases [solid line in Fig. 9(a)]. The effective viscosity for a stationary flow (with neglect of the relaxation time) is plotted as dashed line. It is seen that the deviations of the orientational distribution from equilibrium result in a decrease of the real part of the effective viscosity. This implies that the energy is dissipated weaker, and that consequently a_c is lower than in the case of zero relaxation time. The comparison of the solid curve with the dotted ones in Fig. 9(b) shows that the maximum of the imaginary part of the effective viscosity is caused by the long chains.

A comparison of the contributions of chains of different size is done in Fig. 10 for three values of the wave frequency. The size distribution of chains (1) is presented with filled circles in part (a) of that figure. It is seen that at low frequencies ($f = 1$ Hz) the viscoelastic effect is mainly caused by very long chains with small values of g_n [see maximum of $-\text{Im}(\eta_{\text{eff}n})$ at $n = 16$ in Fig. 10(b)]. For $f = 5$ Hz the maximum of $-\text{Im}(\eta_{\text{eff}n})$ is shifted to long chains ($n = 11$) and the value of the maximum in-

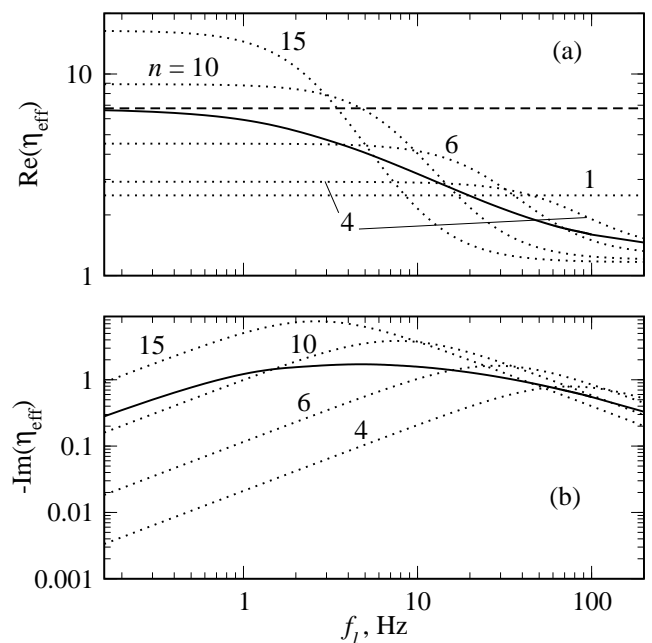


FIG. 9: The dependencies of the real (a) and the imaginary (b) part of the effective viscosity on the wave frequency. The dashed line denotes the effective viscosity, which is calculated with neglect of the relaxation time for $\varepsilon = 5$. The solid lines denote the effective viscosity calculated using the size distribution of chains (1), and the dotted curves present the real and imaginary parts of the effective viscosity for model ferrofluids containing chains of n particles only. $H_0 = 0$, the remaining parameters are the same as before.

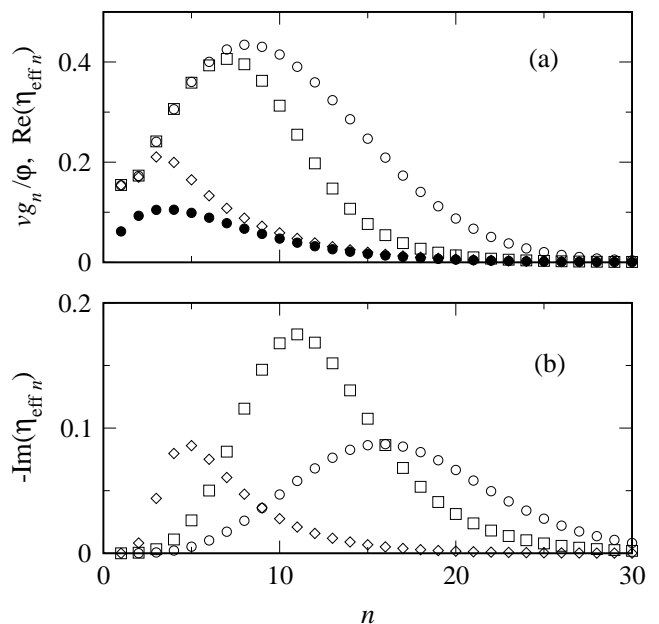


FIG. 10: Contributions of chains containing n particles in the real (a) and in the imaginary part (b) of the effective viscosity at $f_l = 1$ Hz (\circ), 5 Hz (\square), and 100 Hz (\diamond). The filled circles present the size distribution of chains (1). The remaining parameters are the same as in Fig. 9.

creases. Together with the larger values of g_n for those long chains, the total viscoelastic effect is larger than for $f = 1$ Hz [compare the area under the \circ - and \square -curve in Fig. 10(b)]. For high frequencies as $f = 100$ Hz the maximum of $-\text{Im}(\eta_{\text{eff}n})$ is at short chains ($n = 5$) and the value of the maximum decreases. This decrease cannot be compensated by the even larger values of g_n for those short chains. Thus the total viscoelastic effect decreases again: the area under the \diamond -curve is smaller than the area under the \square -curve.

In summary, by increasing the frequency from 1 to 100 Hz the viscoelastic effect passes at maximum at $f = 5$ Hz [solid curve in Fig. 9(b)]. The maximal contribution to $-\text{Im}(\eta_{\text{eff}n})$ comes for $f \lesssim 100$ Hz from chains off the maximum of g_n . Comparing the area under the \circ -, \square -, and \diamond -curve in Fig. 10(a), one can see that the area is continuously shrinking with f . It results in the solid line in Fig. 9(a) describing the weaker dissipation of energy in the system.

The origin of the viscoelasticity (i. e., the dependence of the relation between the tensors of velocity gradients and the stress tensor on the history) in a ferrofluid with chains can be explained in the following way. When the orientation of a chain is changed from the equilibrium by the velocity gradients, a restraining moment is generated by the applied field. Thus the network of chains is an "elastic" element of the system, which interacts with the viscous carrier liquid. If the relaxation time of a chain is much shorter than the period of the vibrations, the orientation of chains and consequently the rheological properties of the suspension do not depend on history, and there is no viscoelastic properties. This fact becomes more obvious, if one notes that the relaxation time of a chain is proportional to the carrier liquid viscosity. Thus the negligible relaxation time of a chain implies a weak coupling between the chain and the carrier.

To estimate the importance of the relaxation processes in a ferrofluid with chains, the Deborah number De is calculated for the subharmonic response. The Deborah number is the product of the angular wave frequency with the mean relaxation time of a chain, $De = \omega_l \tau_0$. In the case of polymer solutions, the most pronounced viscoelastic behaviour should be expected in the range of $De \approx 1$, whereas at $De \gg 1$ a recovery of the Newtonian behaviour was observed⁴¹. In the case of ferrofluids with chains, the viscoelastic behaviour is present over a much wider De range. The frequency range of Fig. 9 gives $0.033 \leq De \leq 3.3$ for which a viscoelastic behaviour is present since $-\text{Im}(\eta_{\text{eff}}) \neq 0$. That fact is supported by the range of appearance for the abnormal tongues considered to be a characteristic feature of viscoelastic behaviour. From Fig. 4 one can read that viscoelastic properties can be expected even for De beyond 10.

Obviously the viscoelasticity of a ferrofluid with chains differs from that of a polymer solution. The reason for this difference is the following. The relaxation time of a long polymer chain involved in the polymer dynamics is the conformational relaxation time. As soon as

the period of excitation becomes much shorter than the conformational relaxation time, the polymer chain does not participate in the movement of the solution. Therefore a motion of the Newtonian solvent through the rigid obstacles of polymer chains is observed. In the case of the rather short chains formed by magnetic particles, the relaxation time is the orientational relaxation time of a chain⁴⁹ in the viscous carrier liquid. Since it is proportional to the viscosity of the carrier liquid, the high values of τ_0 and De , respectively, mean a strong coupling between the motion of a chain and the carrier liquid, which ensures the viscoelastic behaviour. Thus ferrofluids widen significantly the range in which viscoelastic features can be observed in contrast to polymer solutions.

In a real ferrofluid, any variation of the system parameters not only varies the Deborah number but also affects the critical parameters either directly or indirectly by changing other properties as permeability or viscosity. In order to investigate the role of the deviations of the chains from equilibrium in greater detail, a model ferrofluid with a tunable coefficient of rotational diffusion for all chains $D_{\text{tune},n} = D_n D_{\text{scale}}$ is studied. Via that coefficient the mean relaxation time τ_0 , i.e. the Deborah number, can be varied.

D_{scale} is a phenomenological parameter, which is related neither to the chain size nor to the fluid properties. Using this phenomenological parameter, a smooth transition can be realized from a model ferrofluid with chains

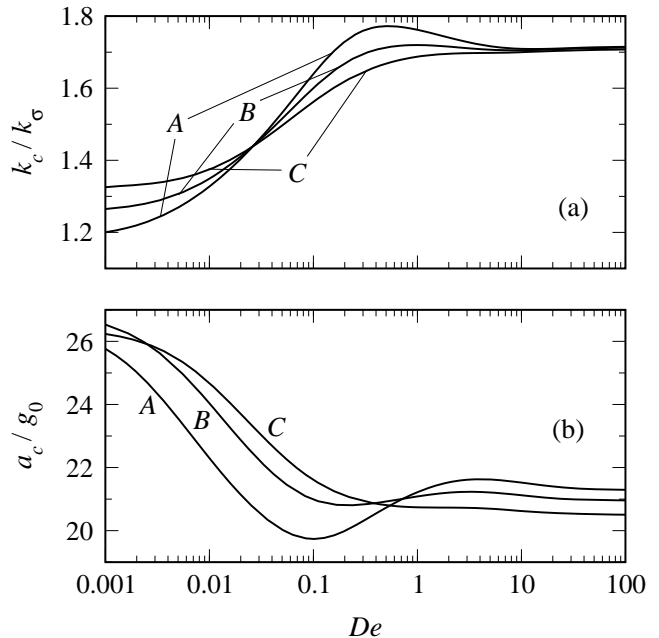


FIG. 11: Dependency of the critical wave number (a) and the critical acceleration amplitude (b) on the Deborah number for a model ferrofluid with the tunable relaxation time of a chain. The coupling constant and the Langevin parameter are: Curves A: $\varepsilon = 5.5$, $\kappa = 0.39$, B: $\varepsilon = 5$, $\kappa = 0.5$, and C: $\varepsilon = 4.5$, $\kappa = 0.63$. The remaining parameters are the same as before.

almost in equilibrium ($D_{\text{scale}} \gg 1$ gives $De \ll 1$) to the real ferrofluid ($D_{\text{scale}} = 1$), and further to a model ferrofluid with chains far from the equilibrium ($D_{\text{scale}} \ll 1$ gives $De \gg 1$).

It is seen in Fig. 11 that even small deviations from equilibrium are significant as the variation of k_c and a_c in the range from $De \sim 0.001$ to $De \sim 0.01$ show. In the case of a system with long chains ($\varepsilon = 5.5$), a pronounced minimum in the dependence of $a_c(De)$ and a maximum in that of $k_c(De)$ are observed. As ε and the mean chain length decrease, these extrema are shifted towards higher values of De and become less pronounced and disappear for $\varepsilon = 4.5$. Beyond $De \sim O(1)$ one observes a saturation of k_c and a_c close to the corresponding extremal values. That means that beyond a certain deviation from equilibrium, viscoelastic effects can neither be enhanced nor diminished. The latter confirms that there is no recovery to a Newtonian behaviour at high De numbers.

V. CONCLUSION

The rheological properties of a ferrofluid caused by the formation of chains is investigated by the linear analysis of the Faraday instability in a horizontal magnetic field. A horizontally unbounded ferrofluid layer of a finite depth has been considered. The dependencies of the critical acceleration amplitude a_c and the critical wave vector on the excitation frequency f , the magnetic field \mathbf{H}_0 , and the dipolar coupling constant ε have been obtained for different depths of the layer in a wide range of fluid viscosities. A viscoelastic behaviour is predicted, which is indicated by the qualitative changes in the neutral stability curve: an abnormal tongue appears which has no tip and upper boundary in contrast to all other tongues (Fig. 2). Beside its existence it is revealed how this abnormal tongues is formed by the merging of other tongues as the viscosity of the carrier liquid is changed

(Fig. 3).

The threshold of the instability depends on the applied field and on the angle θ between the wave vector and the applied field separately (Fig. 7). Therefore one can easily test a ferrofluid whether it contains chains or not by choosing different combinations of θ and H_0 but the same value for $H_0 \cos \theta$. If the ferrofluid contains chains one get different thresholds whereas the surface of a chain-free ferrofluid is destabilized at a unique value of a_c .

A ferrofluid with chains whose orientation is out of equilibrium compared with other model ferrofluids (Figs. 6, 8) has the lowest threshold of all. This is caused by a decrease of the real part of the effective viscosity [Fig. 9(a)] which corresponds to a weaker dissipation of energy and thus to a lower value of a_c . The nonzero imaginary part of the effective viscosity [Fig. 9(b)] indicates also the viscoelastic behaviour of the studied ferrofluid. By analyzing the dependence of the critical parameters on the Deborah number, it is found that a viscoelastic behaviour occurs over a much wider range than in viscoelastic polymer solutions. Particularly no recovery to a Newtonian behaviour at high Deborah numbers is found.

The present model is restricted to the case of a monodisperse ferrofluid. An account of the polydispersity will be necessary to compare the predictions with future experiments using real ferrofluids. The dipolar interactions between chains and their flexibility will influence the properties of a real ferrofluid. Nevertheless, the above-discussed effects should be detectable, at least qualitatively, in a real experiment.

Acknowledgments

The authors have much benefited from stimulating discussions with R. Richter and A. Engel. This work was supported by the Deutsche Forschungsgemeinschaft under Grant No. LA 1182/2-3.

* vladik@mpipks-dresden.mpg.de

† adlange@mpipks-dresden.mpg.de

¹ R. E. Rosensweig, *Ferrohydrodynamics*, Cambridge University Press, Cambridge, 1993.

² P. G. de Gennes and P. A. Pincus, *Pair correlations in a ferromagnetic colloid*, Phys. Kondens. Mater. **11**, 189 (1970).

³ P. C. Jordan, *Field-dependent chain formation by ferromagnetic colloids*, Mol. Phys. **38**, 769 (1979).

⁴ S. Taketomi, H. Takashi, N. Inava, and H. Miyajima, *Experimental and theoretical investigations on aggregation of magnetic particles in magnetic fluids*, J. Phys. Soc. Jpn. **60**, 1689 (1991).

⁵ V. M. Buzmakov and A. F. Pshenichnikov, *On the structure of microaggregates in magnetite colloids*, J. Colloid Interface Sci. **182**, 63 (1996).

⁶ R. B. Bird, *Usefull non-Newtonian models*, Annu. Rev. Fluid Mech. **8**, 13 (1976).

⁷ R. B. Bird, *Constitutive equations for polymeric liquids*, Annu. Rev. Fluid Mech. **27**, 169 (1995).

⁸ M. Doi and S. F. Edwards, *The theory of polymer dynamics*, Oxford University Press Inc., New York, 1986.

⁹ J. L. Ericksen, *Anisotropic fluids*, Arch. Rational Mech. Anal. **4**, 231 (1960).

¹⁰ J. L. Ericksen, *Theory of anisotropic fluids*, T. Soc. Rheol. **6**, 29 (1960).

¹¹ F. M. Leslie, *Some constitutive equations for anisotropic fluids*, Q. J. Mech. Appl. Math. **19**, 357 (1966).

¹² O. Parodi, *Stress tensor for a nematic liquid crystal*, J. Phys. (Paris) **31**, 581 (1970).

¹³ F. M. Leslie, *An analysis of a flow instability in nematic liquid crystals*, J. Phys. D **9**, 925 (1976).

¹⁴ M. Simões, A. J. Palagana, and L. R. Eangelista, *Unstable periodic structures in nematic liquid crystals*, Braz. J. Phys. **28**, 348 (1998).

¹⁵ F. M. Leslie, *Magnetohydrodynamic effects in the nematic*

- mesophase*, Chem. Phys. Lett. **13**, 368 (1972).
- ¹⁶ M. G. Clark and F. M. Leslie, *A calculation of orientational relaxation in nematic liquid crystals*, Proc. R. Soc. London, Ser. A **361**, 463 (1978).
- ¹⁷ P. G. de Gennes, *Physics of liquid crystals*, London: Oxford UP, 1974.
- ¹⁸ S. Chandrasekhar, *Liquid crystals*, Cambridge University Press, 1977.
- ¹⁹ V. N. Pokrovskij, *Stresses, viscosity, and optical anisotropy of a moving suspension of rigid ellipsoids*, Soviet Physics Uspekhi-USSR **14**, 737 (1972).
- ²⁰ V. N. Pokrovskij, *Statistical Mechanics of the dilute suspensions*, Nauka, Moscow, 1978.
- ²¹ R. Hanaoka, S. Takata, H. Fujita, T. Fukami, K. Sakurai, K. Isobe, and T. Himo, *Electroviscoelastic properties in ER gel of disperse system under DC electric field*, Int. J. Mod. Phys. B **16**, 2433 (2002).
- ²² Y. An, B. Liu, and M. Shaw, *Soft gels with ordered iron particles: fabrication and electroviscoelastic response*, Int. J. Mod. Phys. B **16**, 2440 (2002).
- ²³ G. Bossis, S. Lacis, A. Mainer, and O. Volkova, *Magnetorheological fluids*, J. Magn. Magn. Mater. **252**, 224 (2002).
- ²⁴ A. Y. Zubarev and L. Y. Iskakova, *Effect of chainlike aggregates on dynamical properties of magnetic liquids*, Phys. Rev. E **61**, 5415 (2000).
- ²⁵ M. Faraday, *On the forms and states assumed by fluids in contact with vibrating elastic surfaces*, Philos. Trans. R. Soc. London **52**, 319 (1831).
- ²⁶ H. W. Müller, H. Wittmer, C. Wagner, J. Albers, and K. Knorr, *Analytic stability theory for Faraday waves and the observation of the harmonic surface response*, Phys. Rev. Lett. **78**, 2357 (1997).
- ²⁷ W. S. Edwards and S. Fauve, *Pattern and quasi-patterns in the Faraday experiment*, J. Fluid Mech. **278**, 123 (1994).
- ²⁸ H. W. Müller, *Periodic triangular patterns in the Faraday experiment*, Phys. Rev. Lett. **71**, 3287 (1993).
- ²⁹ A. Kudrolli, B. Pier, and J. P. Gollub, *Superlattice patterns in surface waves*, Physica D **123**, 99 (1998).
- ³⁰ H. Arbell and J. Fineberg, *Spatial and temporal dynamics of two interacting modes in parametrically driven surface waves*, Phys. Rev. Lett. **81**, 4384 (1998).
- ³¹ H. Arbell and J. Fineberg, *Two-mode rhomboidal states in driven surface waves*, Phys. Rev. Lett. **84**, 654 (2000).
- ³² K. Kumar and L. Tuckerman, *Parametric instability of the interface between two fluids*, J. Fluid Mech. **279**, 49 (1994).
- ³³ J. Bechhoefer, V. Ego, S. Manneville, and B. Johnson, *An experimental study of the onset of parametrically pumped surface waves in viscous fluids*, J. Fluid Mech. **288**, 325 (1995).
- ³⁴ E. Cerda and E. Tirapegui, *Faraday's instability for viscous fluids*, Phys. Rev. Lett. **78**, 859 (1997).
- ³⁵ O. Lioubashevski, J. Fineberg, and L. S. Tuckerman, *Scaling of the transition to parametrically driven surface waves in highly dissipative systems*, Phys. Rev. E **55**, R3832 (1997).
- ³⁶ S. Kumar, *Mechanism for the Faraday instability in viscous liquids*, Phys. Rev. E **62**, 1416 (2000).
- ³⁷ V. V. Mekhonoshin and A. Lange, *Faraday instability on viscous ferrofluids in a horizontal magnetic field: Oblique rolls of arbitrary orientation*, Phys. Rev. E **65**, 061509 (2002).
- ³⁸ C. Wagner, H. W. Müller, and K. Knorr, *Faraday waves on a viscoelastic liquid*, Phys. Rev. Lett. **83**, 308 (1999).
- ³⁹ H. W. Müller and W. Zimmermann, *Faraday instability in a linear viscoelastic fluid*, Europhys. Lett. **45**, 169 (1999).
- ⁴⁰ S. Kumar, *Parametrically driven surface waves in viscoelastic liquids*, Phys. Fluids **11**, 1970 (1999).
- ⁴¹ S. Kumar, *Vibration-induced interfacial instabilities in viscoelastic fluids*, Phys. Rev. E **65**, 026305 (2002).
- ⁴² There is a misprint in²⁴ and²⁰. In the expression for $\chi_n \alpha'_0$ has to be in the denominator of the first fraction.
- ⁴³ H. W. Müller, *Parametrically driven surface waves on viscous ferrofluids*, Phys. Rev. E **58**, 6199 (1998).
- ⁴⁴ T. Völker and S. Odenbach, *The influence of a uniform magnetic field on the Soret coefficient of magnetic nanoparticles*, Phys. Fluids **15**, 2198 (2003).
- ⁴⁵ P. Chen and J. Viñals, *Pattern selection in Faraday waves*, Phys. Rev. Lett. **79**, 2670 (1997).
- ⁴⁶ P. Chen and J. Viñals, *Amplitude equation and pattern selection in Faraday waves*, Phys. Rev. E **60**, 559 (1999).
- ⁴⁷ In Ref. 40 the term 'broad harmonic tongue' was used. To the authors opinion that term does not note clearly enough the difference to all other tongues.
- ⁴⁸ M. A. Martsenyuk, Y. L. Raikher, and M. I. Shliomis, *Kinetics of magnetization of suspensions of ferromagnetic particles*, Zh. Exp. Teor. Fiz. **65**, 834 (1974).
- ⁴⁹ The estimation for the ratio of the kinematic energy of the chain rotation and the thermal energy gives 10^{-8} for a chain containing 5 particles and $f = 100$ Hz, therefore, inertia of a chain is neglected.